



Experimental analysis of transport characteristics for vertically aligned carbon nanotube membranes

Seung Min Park^a, Young-Kwon Choi^a, Sangho Lee^{a,*}, Youngbin Baek^b, Jeyong Yoon^b, Dong Kyun Seo^c, Yong Hyup Kim^c

^aDepartment of Civil and Environment Engineering, Kookmin University, Jeongneung-gil 77, Seongbuk-gu, Seoul 136-702, Republic of Korea

Tel. +82 2 910 5060; Fax: +82 2 910 8597; email: sanghlee@kookmin.ac.kr

^bSchool of Chemical and Biological Engineering, Seoul National University, Seoul, Republic of Korea

^cSchool of Mechanical and Aerospace Engineering, Seoul National University, Seoul, Republic of Korea

Received 15 June 2012; Accepted 28 September 2012

ABSTRACT

Membranes utilizing carbon nanotubes (CNTs) as their pores have been emerged as a novel technique for water and wastewater treatment. CNTs are nanometer-diameter cylinders, allowing fast transport of water molecular and other fluid due to their strong hydrophobic characteristics. A few studies have been done for developing membranes embedding single-wall or multiwall nanotubes and simulating their performance theoretically using molecular dynamics. Nevertheless, only a limited number of experimental works were attempted to analyze the transport phenomena inside the CNT membranes due to lack of techniques for quantitative interpretation of the experimental results. Accordingly, this study aimed at developing protocols to quantify the efficiency of CNT membranes and apply them for better understanding of transport mechanisms of the CNT membranes. Membranes made of vertically aligned CNTs, which has 3–5 nm inner diameter and 150~250 μm length, were used. Special experimental techniques were applied to obtain reliable data from the CNT membranes having small surface areas (less than 0.1 cm²). The slip-modified Hagen–Poiseuille equation was applied to analyze flux enhancement for the CNT membranes.

Keywords: Vertically aligned carbon nanotube; CNT membrane; Slip-modified Hagen–Poiseuille equation; The enhancement factor; Filtration model

1. Introduction

There is a continuous increase in the demand for water because of the growth in population and the

growth in industries. Water supplies everywhere are also under threat from climate change. Accordingly, water shortage exists in many areas of the world and is likely to become more severe in future years. A potential solution for this problem is to use alternative water resources such as seawater, brackish water, and

*Corresponding author.

reclaimed wastewater. Unlike conventional water resources such as river water and groundwater, the amount of alternative water resources is sufficient for human use.

Unfortunately, the ability to exploit these resources is currently limited by the lack of technologies, which have affordable energy consumption with high treatment efficiency. Reverse osmosis (RO) is widely used for the production of fresh water from the alternative water resources. Nevertheless, current RO membranes require improvement in their water permeability in order to reduce energy consumption.

One of the technologies that hold promise is the RO membranes using carbon nanotubes (CNTs) as their pores. CNTs are unique and one-dimensional macromolecules that have outstanding thermal and chemical stability. These nano-materials have been proven to possess good potential as superior characteristic. In the CNT RO membranes, strong hydrophobic characteristics of CNT inner wall accelerate the transport of water molecules, allowing high flux and low-energy consumption for water treatment.

A few works have been attempted to use CNT for membrane synthesis. CNT membranes that have much higher water permeability than conventional membranes were prepared by different methods [1–6]. The potential of the CNT membranes for various applications has been investigated, including programmable transdermal drug delivery of nicotine [7], biomolecule separation, chemical separation [8], DNA translocation [9], water desalination [10], and natural protein channel mimicking and gas separation [11].

Studies have been also performed to understand the water transport through the CNT membranes. Pressure driven flow velocities of three to five orders of magnitude higher than predicted from Newtonian Flow using the Hagen–Poiseuille equation has been observed in multiwalled carbon nanotube (MWNT) membrane pores [11,12]. Molecular dynamics (MD) simulations have been applied to interpret the increased water flow through CNTs [13,14]. As a result of such works, it was found that liquid flow through CNT with diameters as small as ~ 2 nm can be described using the slip-modified Hagen–Poiseuille equation [13].

In this article, we focused on the development of techniques for quantitative analysis of CNT membrane performance and water transport mechanisms. Membranes consisting of vertically aligned CNTs, which has 3–5 nm inner diameter and 150–250 μ m length, were used. The slip-modified Hagen–Poiseuille equation was applied for theoretical analysis of flux enhancement for the CNT membranes.

2. Theory

The water transport through a porous membrane is commonly described by the continuum hydrodynamics model such as the Hagen–Poiseuille equation.

$$Q_{\text{HP}} = \frac{\pi \left(\frac{d}{2}\right)^4}{8\mu} \frac{\partial p}{\partial z} \quad (1)$$

where Q_{HP} is the volumetric flow rate, ∂P is the pressure drop, d is the pore diameter, μ is the water viscosity, and ∂z is the membrane thickness.

In a CNT membrane, water flow rate may exceed the predicted values from the continuum hydrodynamics model. The non-slip boundary condition cannot be applied to the inner wall of CNT because it allows slip motion of water molecules due to reduced interaction by the hydrophobic nature of the graphene-like structures. Accordingly, the slip-modified Hagen–Poiseuille equation should be applied to predict water flow rate inside the CNT [1].

$$Q_s = \frac{\pi \left[\left(\frac{d}{2}\right)^4 + 4\left(\frac{d}{2}\right)^3 L_s \right]}{8\mu} \frac{\partial p}{\partial z} \quad (2)$$

where L_s is defined as the slip length, the slip length was predicted by a flat graphene sheet [14].

$$L_s(d) = L_{s,\infty} + \frac{c}{d^3} \quad (3)$$

where $L_{s,\infty}$ ($=30$ nm) is the slip length over a flat graphene sheet and C is a fitting parameter.

The water viscosity decreases with decreasing CNT diameter. Inside smaller CNTs, the effective water viscosity is smaller due to the increased ratio of interface to bulk-like area. Although theoretical prediction of water viscosity inside CNT is difficult, we obtained a simple equation by non-linear regression of MD simulation data [13].

$$\mu = 0.5169 + 0.5653 \times \frac{d}{d + 4.9345} \quad (4)$$

This relationship is valid at $1.6 < d < 50$ nm with $R^2 = 0.997$.

Using RO filtration data, the slip lengths can be experimentally determined, which were calculated using a rearranged form of Eq. (2).

$$L_{s,\text{experiment}} = \frac{16Q_s\mu}{\pi d^3} \frac{\partial z}{\partial p} - \frac{d}{8} \quad (5)$$

3. Experimental materials and methods

3.1. CNT membranes

MWNT were synthesized using a chemical vapor deposition (CVD) methods, which were previously reported in literature [15]. Then, CNT forests were filled using epoxy. The reason for using epoxy is to ensure high physical strength against high pressure for membrane filtration. In the preliminary tests, we have tried using several polymeric materials and found that epoxy has enough hardness to fix the vertically aligned CNTs forest. After that, vacuum filtration duration 30 min for suction off air bubble in epoxy. The tip of CNT was removed using a microtome equipped with a glass knife. Examination of many such TEM images revealed that the samples consist mainly of MWNT with the average inner diameter of 4.87 ± 0.87 nm and outer diameter of 7.1 ± 0.88 nm. The thickness of the CNT membranes was calculated from the scanning electron micrograph (SEM) image, which was around 200 μm . The detailed property of the CNT membrane is summarized in Table 1.

3.2. RO filtration

Experiments were performed in batch mode using a stirred cell similar to those which have been widely used for the study of the flux in water research group [17]. The stirred cell shown in Fig. 1 was made of stainless steel. Although the diameter of the stirred cell was 5.1 cm, it is specially designed to test small-size membranes with the effective membrane area of less than 10 mm. The working volume of the stirred cell was 100 mL. The working pressure that was drive water through the CNT membrane as the driving force was provided by a nitrogen cylinder with a gas pressure regulator. The permeate flux was measured using an electronic balance (ARG423, Ohaus, USA) connected to a desktop computer.

The experiments were performed under different pressures including 2, 5, 10, and 20 bar. Only D.I. water was used as the feed solution. Prior to each test, high pressure nitrogen gas was applied to the CNT membrane to remove possible water moisture inside

CNT pores. Then, the water flux was measured at 2 bar. The tests were repeated until stable results were obtained.

4. Results and discussion

Fig. 2 illustrates the SEM images of RO membranes made of CNTs. Due to the limited resolution of the SEM equipment, it was impossible to identify the CNT pores on the membrane surface (Fig. 2(a)). Nevertheless, no defects were observed from these images. The CNT membrane had symmetric structures with the average thickness of 200 μm as confirmed by the SEM images (Fig. 2(b)).

Using these membranes, RO filtration tests were carried out under different pressures as shown in Fig. 3. The water flux ranges from 2,000 to 50,000 L/m²-h, which are higher values than those reported by conventional NF and RO membranes. Nevertheless, direct comparison is not possible at this point because these membranes may not have different rejection capability. As shown in Fig. 4, the flux was proportional to the applied pressure. The average water permeability was calculated to 1,376 L/m²-h-bar. This suggests that the CNT membrane can hold pressure up to 20 bar.

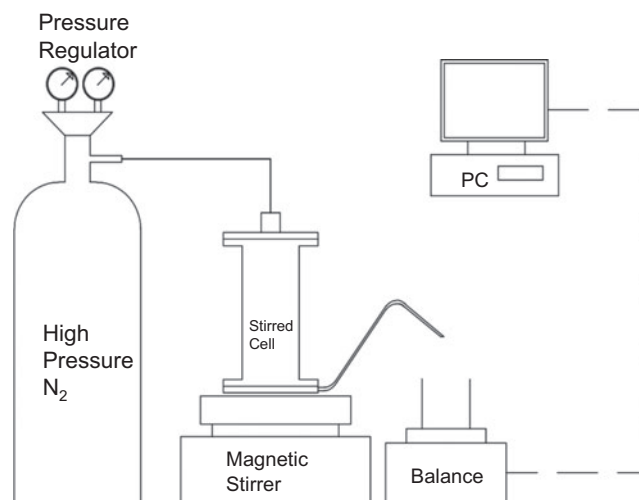


Fig. 1. Schematic diagram of batch RO filtration system.

Table 1
Property of the CNT membrane

Membrane	CNT structure	CNT layer thickness (μm)	CNT areal density (cm^{-2})	CNT outer diameter (nm)	Pore diameter (nm)	CNT tortuosity factor (τ)
Epoxy	MWNT	150–250	2.0×10^{11}	7.1 ± 0.88	4.8 ± 0.87	1

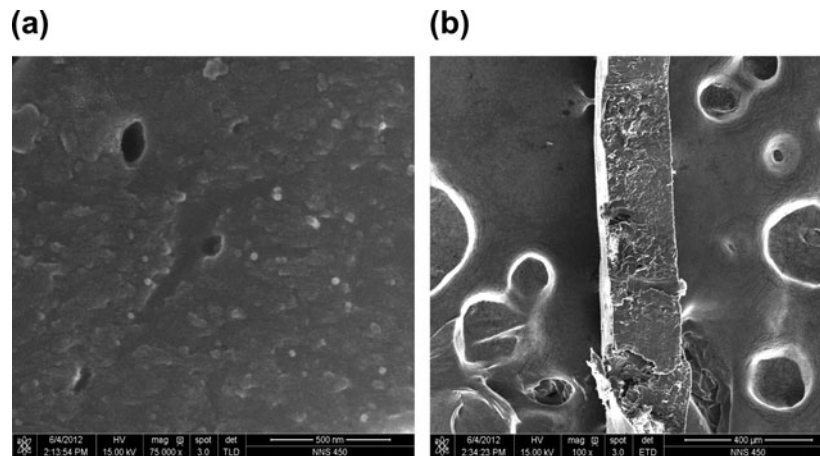


Fig. 2. SEM images of the CNT membrane (a) top and (b) cross-section.

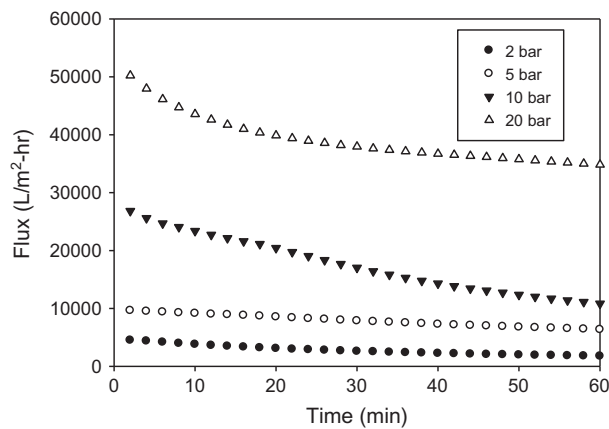


Fig. 3. Changes in water flux through the CNT membrane with time.

It should be noted that the flux continuously decreased even though D.I. water was used as the feed water. Similar results were also reported in the literature [16]. There are several possible reasons for this phenomenon. First, the inner wall of CNT may be wetted by water molecules, leading to a reduced effect of “slipping”. Second, the inlet of CNT pores may be blocked by impurities. Although D.I. water was used, there may be nano-scale impurities affecting the permeability of the CNT membranes. It is unlikely that there were irreversible changes of pore structure. This is because the permeability of the CNT membranes was recovered after N_2 blowing. Further studies should be carried out to identify the mechanisms of flux decline in the CNT membranes.

Using Eq. (5) and the data in Fig. 3, the slip lengths were estimated at different pressures. As illustrated in Fig. 5, the slip lengths ranged from 10,000 to 23,000 nm. Considering the size of error bars,

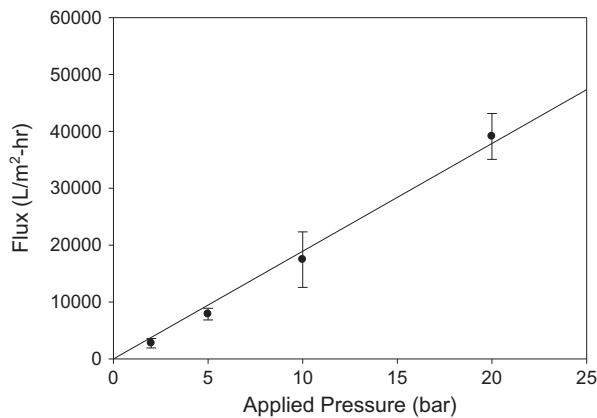


Fig. 4. Dependence of water flux through the CNT membrane on applied pressure.

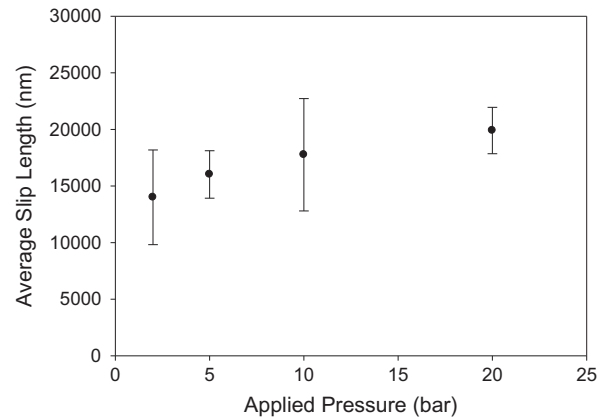


Fig. 5. Estimation of slip lengths under different pressure conditions.

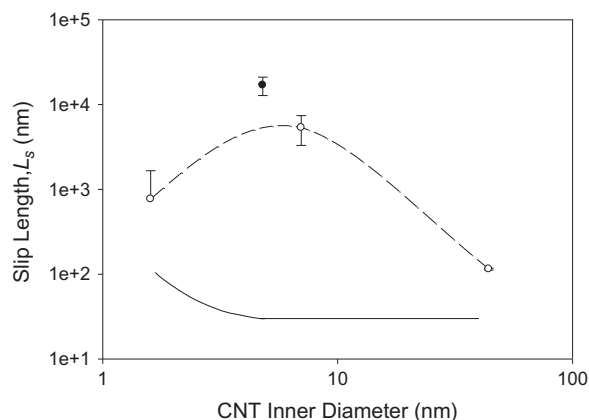


Fig. 6. Comparison of slip length in this study with reported values in the literature.

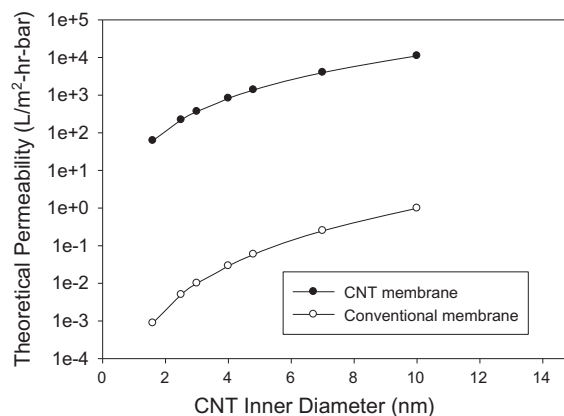


Fig. 8. Comparison of theoretical permeabilities for CNT membrane with those for conventional membranes.

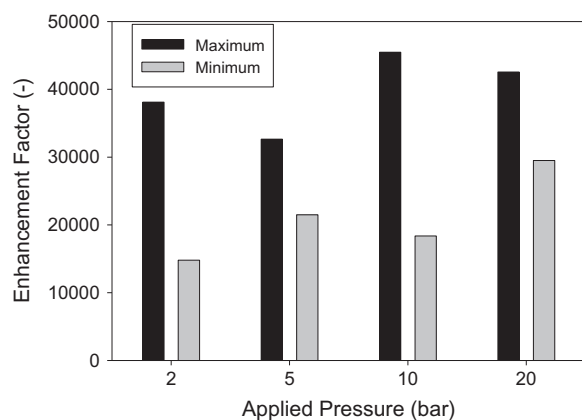


Fig. 7. The maximum and minimum enhancement factors of water flux from model calculations and experimental data.

it is likely that the slip length did not depend on the applied pressure. The average slip length for the CNT membrane was determined to be 16,000 nm.

The slip length of the CNT membranes in this study was compared with those in the literature. The broken line indicates the reported values from experimental works [1,11,12], while the solid line indicates the predicted values from MD simulation [13]. Using the 1.66 nm CNT, Thomas et al. [13] present the flow rate enhancement is 433. Holt et al. [1] present the enhancement factor is 560 to 9,600. According to Majumder et al. [12], the flow enhancement through 7 nm diameter, are 10,000 to 100,000. Considering the CNT size in this study, it is likely that the slip length in this study has similar value to the values in previous experiments. Further works should be done to check whether there is an additional flow to the

water flow inside CNT. Although the data are not shown, the rejection tests using silica nanoparticles suggest that there is no such flow. Nevertheless, it is necessary to test these membranes under a variety of different conditions. The effect of slip length on the water flux can be quantitatively expressed by the enhancement factor, which is defined as the ratio of the measured flow rate (Q_s) to theoretical flow rate (Q_n).

$$\varepsilon = \frac{Q_s}{Q_n} \quad (6)$$

where Q_s is the volumetric flow rate with slip and Q_n is the non-slip Hagen–Poiseuille flow rate that was obtained by setting L_s equal to zero. Fig. 6 shows the maximum and minimum enhancement factors at different pressures. The difference between maximum and minimum values was larger at 2 bar and 10 bar than at 5 bar and 20 bar, suggesting the rate of wetting is not proportional to the applied pressure (Fig. 7).

In Fig. 8, the water permeability of the CNT membranes was simulated for different inner diameters of CNT using the slip length obtained in the experiments. The results suggest that the water permeability increased by several order of magnitudes with increasing the CNT size. If the CNT with inner diameter of 1.6 nm are used, which may be necessary to increase solute rejection, the water permeability of the CNT membranes decrease to 62 L/m²-h-bar.

5. Conclusions

In this study, the fundamental characteristics of CNT membranes were investigated and the following conclusions were drawn:

- (1) The CNT membranes with average pore size of 4.87 nm and average thickness of 200 nm were synthesized and tested. The average water permeability was 1,376 L/m²-h-bar.
- (2) Although D.I. water was used, flux decline was observed with time. This is probably because of pore wetting or inlet blocking of CNT. No irreversible changes were observed.
- (3) Water flux through the CNT membranes was interpreted by introducing the concept of “slip length” into the classical Hagen–Poiseuille model. The slip lengths range from 10,000 to 23,000 nm, depending on the test conditions. These values were comparable with the results from other research groups [11,12]. The enhancement factor calculated from Eq. (5) was between 15,000 and 45,000.
- (4) Simple simulation results suggest that the water permeability is dramatically reduced by decreasing CNT pore size. This suggests that the CNT membranes with higher rejection may have much smaller water permeability even with same slip length.

Acknowledgment

This study was supported by the CNT Membrane R and D Project funded by the K-water and the National Research Foundation of Korea Grant funded by the Korean Government (MEST) (NRF-2010-0029061).

References

- [1] J.K. Holt, H.G. Park, Y. Wang, M. Stadermann, A.B. Artyukhin, C.P. Grigoropoulos, A. Noy, O. Bakajin, Fast mass transport through sub-2-nanometer carbon nanotubes, *Science* 312 (2006) 1034–1037.
- [2] K.B. Jirage, J.C. Hulteen, C.R. Martin, Nanotubule-based molecular-filtration membranes, *Science* 278 (1997) 655–658.
- [3] C.R. Martin, M. Nishizawa, K. Jirage, M.S. Kang, S.B. Lee, Controlling ion-transport selectivity in gold nanotubule membranes, *Adv. Mater.* 13 (2001) 1351–1362.
- [4] S.A. Miller, V.Y. Young, C.R. Martin, Electroosmotic flow in template-prepared carbon nanotube membranes, *J. Am. Chem. Soc.* 123 (2001) 12335–12342.
- [5] E.D. Steinle, D.T. Mitchell, M. Wirtz, S.B. Lee, V.Y. Young, C. R. Martin, Ion channel mimetic micropore and nano-tube membrane sensors, *Anal. Chem.* 74 (2002) 2416–2422.
- [6] S.B. Lee, D.T. Mitchell, L. Trofin, T.K. Nevanen, H. Soderlund, C.R. Martin, Antibody-based bio-nanotube membranes for enantiomeric drug separations, *Science* 296 (2002) 2198–2200.
- [7] J. Wu, K.S. Paudel, C. Strasinger, D. Hammell, A.L. Stinchcomb, B.J. Hinds, Programmable transdermal drug delivery of nicotine using carbon nanotube membranes, *Proc. Natl. Acad. Sci. U. S. A.* 107 (2010) 11698–11702.
- [8] X. Sun, X. Su, J. Wu, B.J. Hinds, Electrophoretic transport of biomolecules through carbon nanotube membranes, *Langmuir* 27 (2011) 3150–3156.
- [9] H. Liu, J. He, J. Tang, H. Liu, P. Pang, D. Cao, P. Krstic, S. Joseph, S. Lindsay, C. S. Nuckolls, Translocation of single-stranded DNA through single-walled carbon nanotubes, *Science* 327 (2010) 64–67.
- [10] F. Fornasiero, H.G. Park, J.K. Holt, M. Stadermann, C.P. Grigoropoulos, A. Noy, O. Bakajin, Ion exclusion by sub-2-nm carbon nanotube pores, *Proc. Natl. Acad. Sci. U. S. A.* 105 (2008) 17250–17255.
- [11] M. Majumder, A. Stinchcomb, B.J. Hinds, Towards mimicking natural protein channels with aligned carbon nanotube membranes for active drug delivery, *Life Sci.* 86 (2010) 563–568.
- [12] M. Majumder, N. Chorpra, B.J. Hinds, Effect of tip functionalization on transport through vertically oriented carbon nanotube membranes, *J. Am. Chem. Soc.* 127 (2005) 9062–9070.
- [13] J.A. Thomas, A.J.H. McGaughey, K.A. Ottoleo, Pressure-driven water flow through carbon nanotubes insights from molecular dynamics simulation, *Int. J. Therm. Sci.* 49 (2010) 281–289.
- [14] A. John, J.A. Thomas, A.J.H. McGaughey, Reassessing fast water transport through carbon nanotubes, *Nano Lett.* 8 (2008) 2788–2793.
- [15] Q. Hang, Q. Cheng, L. Jie, Synthesis of uniform double-walled carbon nanotubes using iron disilicide as catalyst, *Nano Lett.* 7 (2007) 2417–2421.
- [16] M. Majumder, B. Corry, Anomalous decline of water transport in covalently modified carbon nanotube membranes, *Chem. Commun.* 47 (2011) 7683–7685.
- [17] S. Lee, R.M. Lueptow, Reverse osmosis filtration for space mission wastewater: Membrane properties and operating conditions, *J. Membr. Sci.* 182 (2001) 77–90.